Chemical Geology 290 (2011) 67–74

Contents lists available at SciVerse ScienceDirect

Chemical Geology

journal homepage: www.elsevier.com/locate/chemgeo

Research paper

Co-variation of Mg and C isotopes in late Precambrian carbonates of the Siberian Platform: A new tool for tracing the change in weathering regime?

Boris G. Pokrovsky [a], Vasileios Mavromatis [b,*], Oleg S. Pokrovsky [b]

[a] Geological Institute, Russian Academy of Science, Pyzhevsky Per, 7, 119017, Moscow, Russia
[b] Geosciences and Environment Toulouse (GET), CNRS, UMR 5563, Observatoire Midi-Pyrénées, 14 Avenue Edouard Belin, 31400 Toulouse, France

ARTICLE INFO

Article history:
Received 30 March 2011
Received in revised form 4 August 2011
Accepted 27 August 2011
Available online 3 September 2011

Editor: J.D. Blum

Keywords:
Magnesium
Carbon
Isotopes
Dolomite
Precambrian
Weathering

ABSTRACT

This study reports significant Mg isotopic variations in 32 samples of late Precambrian dolomites from various parts of the Siberian Platform exhibiting a range of $\delta^{13}C$ from −10‰ to +6‰ (V-PDB). In the Ediacaran dolomites from the N and NE part of the Patom Paleobasin, a systematic increase of $\delta^{26}Mg$ from -2.3 ± 0.2‰ to -0.8 ± 0.3‰ (DSM3) along with a $\delta^{13}C$ decrease from +6‰ to −10‰ ($\delta^{26}Mg = -0.072 \times \delta^{13}C - 1.83$) with a correlation coefficient of $R^2 = 0.73$ ($n = 20$) are observed. Within the stratigraphic sequence of Ediacaran and Ediacaran–Lower Cambrian transition successions, all positive C-isotope excursions co-vary with negative Mg-isotope shifts and vice versa. Other samples from the Siberian Platform lay on this regression with $R^2 = 0.66$ ($n = 28$) except for 4 samples, probably diagenetic dolostones, that exhibit a positive $\delta^{26}Mg$–$\delta^{13}C$ correlation. The enrichment of sedimentary dolomite in heavy carbon and light Mg isotopes may be interpreted as a result of a complex interplay of contrasting sedimentation conditions (sea regression versus sea transgression regime) yielding different weathering regimes and relative contributions of carbonate versus silicate rocks. The enrichment of both oceanic water and carbonate sediments by ^{26}Mg could occur during transgression and would coincide with sedimentation of low-^{13}C carbonates, whereas sedimentation of the depleted in ^{26}Mg, and enriched in ^{13}C carbonates could happen under regression regime when exposed carbonate platforms and coastal planes are subjected to intense weathering.

1. Introduction

Stable carbon, oxygen and sulfur isotope variations in past sedimentary records are among the most powerful tools capable of reconstructing palaeoenvironments of the Earth surface. Recently, a suite of 'non-traditional' stable isotopes (B, Ca, Cu, Fe, Mo, Ni, and Zn) has been added to these "classic" ^{13}C and ^{18}O measurements (Beard et al., 2003; Arnold et al., 2004; Kasemann et al., 2005; Anbar and Rouxel, 2007; Severmann et al., 2008; Kasemann et al., 2010; Silva-Tamayo et al., 2010). Carbon isotope fluctuations in sedimentary carbonates attract special attention because they often coincide with bio-stratigraphic boundaries and could be linked to changes in the global carbon cycle (Ripperdan, 2001). Significant long-term C-isotope events were described in deposits of different ages, but the largest events have been found in strata of Neoproterozoic and Ediacaran–Lower Cambrian boundary age. Since the first reports, approximately 25 years ago (Knoll et al., 1986; Magaritz et al., 1986), of the discovery of anomalous low and high ^{13}C Neoproterozoic carbonate successions in the world, broad discussions about the possible geochemical origin and stratigraphic significance of these strata were stimulated (Burns and Matter, 1993; Pokrovsky and Gertsev, 1993; Vinogradov et al., 1994; Kaufman and Knoll, 1995; Brasier et al., 1996; Pokrovsky, 1996; Hoffman et al., 1998; Pelechaty, 1998; Walter et al., 2000; Des Marais, 2001; Shields et al., 2002; Halverson et al., 2005; Melezhik et al., 2005; Nedelec et al., 2005; Shen et al., 2005; Shields, 2005; Fike et al., 2006; Le Guerroué et al., 2006; Pokrovsky et al., 2006a, b; Jiang et al., 2007; Vieira et al., 2007; Zhu et al., 2007; Vinogradov, 2008; Knauth and Kennedy, 2009; Melezhik et al., 2009; Derry, 2010; Halverson et al., 2010; Le Guerroué and Cozzi, 2010; Pokrovsky et al., 2010).

Magnesium stable isotope analyses were shown to be efficient proxies for carbonate mineral precipitation environments (Galy et al., 2002; de Villiers et al., 2005; Buhl et al., 2007; Immenhauser et al., 2010), although both studies of natural systems and ab-initio calculations have shown limited temperature effect on Mg fractionation (Galy et al., 2002; Schauble, 2010). Until now, Mg-isotopes were used exclusively for contemporary sedimentary and weathering environments (Jacobson et al., 2010) and aimed at establishing the main laws of Mg fractionation in nature. Although these studies are still in progress, it seems important to study in parallel the historical and geological aspects of Mg isotope geochemistry, in particular, their significant potential for understanding past carbonate sedimentary conditions (Tipper et al., 2006a,b).

The aim of this study is to assess the variation of Mg isotopic composition in Precambrian carbonate sediments from the Siberian Platform in order to test the co-variation between Mg- and C-isotopic excursions. We attempted explaining this link from the viewpoint of change in

* Corresponding author. Tel.: +33 5 61 33 25 66; fax: +33 5 61 33 25 60.
E-mail address: mavromat@get.obs-mip.fr (V. Mavromatis).

0009-2541/$ – see front matter © 2011 Elsevier B.V. All rights reserved.
doi:10.1016/j.chemgeo.2011.08.015

sedimentary environment and weathering regime controlled by sea transgression/regression cycles.

2. Study sites and geological background

2.1. Sampling policy

A schematic map of sample locations is given in Fig. 1. Selected geological objects respond to the following two main requirements: 1) the widest range of $\delta^{13}C$ variations and 2) high magnesium concentration (i.e., dolomite or magnesite rock composition). These conditions are met for late Neoproterozoic (Ediacaran) successions in the Patom Paleobasin that encompasses a 700-km-long arc, the Baikal–Patom plateau of South Central Siberia, and they are traced by wells in adjacent parts of the Siberian Platform (Chumakov, 1959; Bobrov, 1979).

According to current geodynamic reconstruction, the Patom Basin during the Late Neoproterozoic was a broad bay at the south of the Paleoasian Ocean that touched the northern coasts of the Paleosiberian continent (Kheraskova et al., 2010). Glacial deposits described as Bolshoy Patom, Nichatka and Dzhemkukan Formations comprise an important marker horizon in the Neoproterozoic sequences of the Patom Paleobasin (Chumakov, 1993, 2011; Chumakov et al., 2011). These strata correspond to the end Cryogenian (or Marinoan) interval of glaciation from 650 Ma to 635 Ma (Chumakov, 2011, Chumakov et al., 2007, 2011). More than 500 $\delta^{13}C$ evaluations are available now for overlaying Ediacaran carbonate-dominated deposits (Pokrovsky and Gertsev, 1993; Pelechaty, 1998; Pokrovsky et al., 2006a; Melezhik et al., 2009; Pokrovsky et al., 2010), and all studied sections exhibit similar carbon isotope curves. The following three units are connected by gradual transitions (from below to top): I) cap carbonate succession with moderately low $\delta^{13}C$ (−2.0‰ to −4.5‰) including typical cap dolomite of 2 m to 2.5 m thickness and overlaying deposits of 30 m to 200 m thickness; II) "dark", often organic-bearing unit with positive $\delta^{13}C$ (from 3.5‰ to 8.6‰); and III) the ultra-low $\delta^{13}C$ (−7.5‰ to −12.5‰) "light" unit corresponding to the "Shuram–Wonoka" event (Melezhik et al., 2009) occurred between 560 Ma and 580 Ma, although its precise dating is lacking (Fike et al., 2006; Le Guerroué et al., 2006).

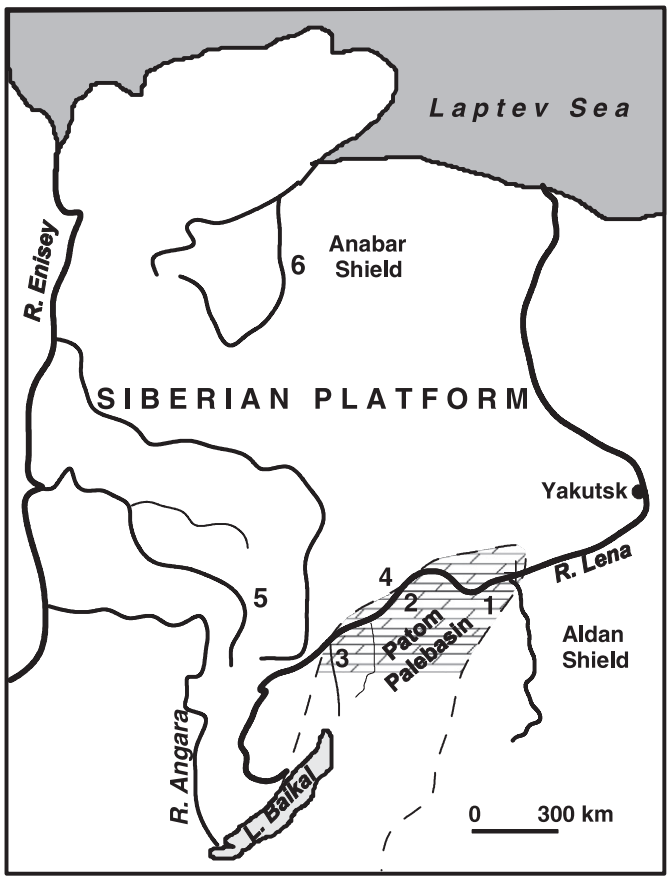

Fig. 1. Schematic map of the studied areas. 1) Northeast of the Patom Paleobasin; 2) North of the Patom Paleobasin 3) West of the Patom Paleobasin; 4) Talakan Rise; 5) Katanga Region; 6) West of the Anabar Shield.

The thicknesses and compositions of unit II and unit III differ in various parts of the paleobasin. In the deep part of the shelf and on the slope of the depression that occupied the central part of paleobasin, the thickness of units II and III reaches 2000 m and 1000 m, respectively, and the contribution of dolomite is minor. Closer to the coast, the thickness of unit II decreases to 400 m to 500 m, and dolomite becomes abundant. In unit III, dolomite only appears on the slope of the Aldan Shield (on the watershed of R. Chara and R. Tokko, borehole lg, Table 1), where it builds up the upper 100 m of the Torgo Formation, which lower 150 m consist of limestone and marls with similar carbon isotope composition (Pokrovsky et al., 2006a).

The Ediacaran–Lower Cambrian boundary at the Patom Paleobasin is not exactly constrained. Dolostone–limestone–sandstone succession (Zherba/Seralakh Formations) that overlays the low-$\delta^{13}C$ unit III was recently dated as Ediacaran (Russian Upper Vendian, (Khomentovskii and Kochnev, 1999), although it was considered as Lower Cambrian in the past (Chumakov, 1959; Salop, 1964). At the NE of Patom Paleobasin the main part of carbonates from Zherba Formation exhibit $\delta^{13}C$ values ranging within 0 ± 2‰, although very low $\delta^{13}C$ (up to −20.1‰) diagenetically altered samples were found among carbonate-bearing sandstones and siltstones (Pelechaty, 1998). At the B. Chuya River (North Part of Patom Paleobasin, series 2 in Fig. 1 and Table 1) the dolostones of Zherba Formation have relatively uniform $\delta^{13}C = 1 \pm 2$‰ with positive excursion up to 6.1‰ (Pokrovsky and Chumakov, 2008). The "normal sea" $\delta^{13}C = 0 \pm 2$‰ values are typical for carbonates of overlaying transition Ediacaran–Lower Cambrian salt-bearing strata (Pelechaty, 1998; Pokrovsky et al., 2006a; Pokrovsky, 2009).

The existence of anhydrite veinlets in limestone and dolostone of the Torgo Formation (Pokrovsky et al., 2006a,b) suggests that the far northeastern part of the basin was subjected to an evaporative regime that was favorable for dolomite sedimentation (Warren, 2000). High $\delta^{18}O$ values (up to 30‰ V-SMOW), low Mn and Sr contents and uniform $\delta^{13}C$ values support a sedimentary origin of the dolostones that were drilled in borehole 1g (Table 1). The dolomites in the western part of unit II probably originated from diagenetic dolomitization of limestones as evidenced by high Mn contents and low $\delta^{18}O$ values (Table 1). The origin of cap dolomites is controversial (see Hoffman, 2011 and Shields, 2005 for a review). Geological and geochemical features of cap dolomites, which appear to conformably sit upon glaciogenic diamictites of the Nichatka Formation (No Sh-100, Table 1) and the Bolshoy Patom Formation (No. 37/05, Table 1), may be explained by the discharge of thawing waters into a partly or completely isolated periglacial basin where dolomite sedimentation occurred according to the dorag model (Pokrovsky et al., 2010).

In addition to the Patom Paleobasin samples, samples of transition strata from the Ediacaran to Cambrian from southwest (R. Katanga region, site 4), north (R. Kotuykan, Anabar shield, site 5) and south (Talakan Rise, just to the north of Patom Paleobasin, site 3) of the Siberian Platform were analyzed. The dolomites from the Katanga region and the Talakan Rise are associated with salts and anhydrites. Two additional dolomite samples of the 500-m-thick Kamo Formation (131/3330, site 4) from the Katanga region and of the 500-m-thick Kotuykan Formation (112-88, site 5) from the Anabar Shield are Early Mezo-Proterozoic (1300–1500 Ma) in age. These samples represent a thick, monotonous dolomite succession of unknown (sedimentary or diagenetic) origin.

The sample of magnesite (122/3028, site 4) was collected from an unusual magnesite–anhydrite rock from the Oskoba Formation that formed in a sabkha (Pustylnikov et al., 1989). At the southwest of the

Table 1
Mg-, C-, O- and Sr-isotope data for Late-Precambrian and Cambrian dolostones of the Siberian Platform and its southern framework.

Hole/deep; № field	Formation (age, unit)	δ^{25}Mg (‰ DSM3)	δ^{26}Mg (‰ DSM3)	δ^{13}C (‰ V-PDB)	δ^{18}O (‰ V-SMOW)	^{87}Sr/^{86}Sr	Mn, ppm	Sr, ppm
North-East of Patom Paleobasin (1)								
2400/3158	Se (E-Cm_1)	−1.03	−2	−0.5	26.9			
1g/275	Tn (E-Cm1)	−0.93	−1.8	−1.4	24.9			
1g/348	Tg (E, u3)	−0.47	−0.89	−9.9	30	0.71034	67	37
1g/354	Tg (E, u3)	−0.66	−1.26	−9.9	27.7		67	34
1g/364	Tg (E, u3)	−0.64	−1.23	−9.7	25.7		59	130
1g/368	Tg (E, u3)	−0.67	−1.3	−9.8	27.8		–	–
1g/384	Tg (E, u_3)	−0.65	−1.23	−10.3	29.2	0.70834	48	24
1g/406	Tg (E, u_3)	−0.26	−0.47	−10	25.3	0.71055	230	140
1g/414	Tg (E, u_3)	−0.44	−0.85	−10.3	23.3		–	–
1g/517	Al (E, u_2)	−1.01	−1.92	−0.95	25.5		680	140
1g/520	Al (E, u_2)	−1.05	−2.02	1.4	22.7		–	–
1g/636	Al (E, u_2)	−0.98	−1.88	5.1	26.6	0.70975	120	64
1g/732	Al (E, u_2)	−0.79	−1.53	3.8	24.5		82	80
2730/1737	Kl (E, u_2)	−1.09	−2.1	3.8	24.3	0.71031	89	52
2730/2490	Kh (E, u_2)	−1.16	−2.23	4.4	27.4	0.71067	225	73
2730/2748	Md (E, u_2)	−1.28	−2.43	5.7	26.5	0.70872	94	63
* Sh-90	Ku (E, u_1)	−1.02	−1.97	−2.2	24.1	0.7124	1711	70
* 37-05	Br (E, u_1)	−1.04	−1.98	−3.5	21.2	0.71651	1250	281
North of Patom Paleobasin (2)								
№ 43/07	Zh (E-Cm_1)	−1.04	−1.87	−0.5	24.5			
№ 99/07	Zh (E-Cm_1)	−1.11	−2.13	6.1	22.8			
West of Patom Paleobasin (3)								
№ 58-08	Ul (E, u_2)	−0.72	−1.38	5.5	21.3		1200	42
№ 56-08	Ul (E, u_2)	−0.48	−0.92	8.6	21.6		1000	43
№ 46-08	Ul (E, u_2)	−0.77	−1.5	4.6	21.8		910	56
№ 45-08	Ul (E, u_2)	−0.55	−1.06	6.8	21.4		650	30
№ 32-08	Gu (E, u_1)	−0.87	−1.65	−4.3	24.6		590	70
№ 29-08	Gu (E, u_1)	−0.6	−1.18	−2.5	23.3		1800	47
Talakan Rise (4)								
17933/109	Bl (Cm_1)	−0.86	−1.62	0.2	21.8			
Katanga region (5)								
122/2863	Kt (E-Cm_1)	−0.72	−1.39	−6.3	24.6			
**122/3028	Os (E-Cm_1)	−0.74	−1.44	−1	26.9			
131/3330	Km (Pt_2)	−1.15	−2.2	1.6	27.8	0.70557		20
West of Anabar Shield (6)								
№ 133-88	Sr (E,)	−0.92	−1.78	−3.4	27.4	0.70844		56
№ 112-88	Um (Pt_2)	−1.19	−2.29	0.5	24.7	0.70488		28

*Cap dolomite; **Magnesite. E — Ediacaran; u_1, u_2, and u_3 — C-isotope units of the Ediacaran sequence (see text for details). Formations: Tn — Tinnaya; Se — Seralakh; Zh — Zherba; Tg — Torgo; Al — Alekseevsk; Kl — Kalancha; Kh — Khalatyrbyt; Md — Moldoun; Ku — Kumakulakh; Br — Barrakun; Ul — Uluntuy; Gu — Goloe Ust'e; Bl — Bilir; Kt — Katanga; Os — Oskoba; Km — Kamo; Sr — Staraya Rechka; Um — Usmastakh. C-, O-, and Sr-isotope data from Pokrovsky and Vinogradov, 1991; Vinogradov et al., 1994; Pokrovsky et al., 2006a; Pokrovsky, 2009; Pokrovsky et al., 2010; and this study.

Siberian Platform, a 10-m- to 25-m-thick magnesite-bearing horizon extends for ~1000 km at a similar stratigraphic level (Krupenin et al., 2008).

All collected dolomite are fine grain rocks without visible traces of strong deep burial diagenetic alterations such as breccia, veins and veinlets, silicification and the presence of large size dolomite crystals. All dolomites are poor in silicate admixtures (<3%) except for cap dolomites No. Sh-90 and 37-05 that contain ~40% and ~10% silicate minerals, respectively. The influence of this admixture on Mg-isotope composition seems to be negligible because terrigenous material mainly consists of Mg-poor quartz and feldspar. The amount of clay minerals was below the detection limit of the XRD analysis (i.e., <1–2%).

2.2. Geochemical background

The reasons for abrupt changes in carbon isotope composition in Neoproterozoic carbonates are still uncertain. High-δ^{13}C carbonates, which are widely distributed all over the world, certainly acquired their isotopic compositions at the sedimentation stage due to a high rate of bio-productivity and organic matter burial in sediments (Kaufman and Knoll, 1995; Jacobsen and Kaufman, 1999; Walter et al., 2000; Des Marais, 2001; Shields et al., 2002; Pokrovsky et al., 2006b). Another important factor of heavy carbonate formation may be the increased ^{13}C input to the ocean due to the exposure and weathering of carbonate platforms during sea level regressions (Shields et al., 2002). The reported negative correlation between δ^{13}C and the ^{87}Sr/^{86}Sr ratio in carbonates of unit II suggests the possibility of a δ^{13}C decrease from strongly positive (~6‰ to 8‰) to moderately positive (2‰ to 4‰) values during diagenesis (Pokrovsky et al., 2006b). The primary low δ^{13}C signal in cap dolomites (unit I) is considered as almost certain, although there are numerous works considering the effect of sedimentation and diagenesis (Knoll et al., 1996; Hoffman et al., 1998; Grotzinger and James, 2000; Kennedy et al., 2001; Jiang et al., 2003; Shields, 2005; Hoffman et al., 2007; Pokrovsky et al., 2010).

Two hypotheses can be cited concerning the origin of the ultra-low δ^{13}C carbonates (unit III). These carbonates are also known in Oman, Australia, and China as the global Shuram–Wonoka event. According to the first hypothesis, these carbonates were formed by sedimentation in seawater enriched by oxidized organic carbon (Melezhik et al., 2005; Fike et al., 2006; Le Guerroué et al., 2006; Pokrovsky et al., 2006a,b; Jiang et al., 2007; Zhu et al., 2007; Melezhik et al., 2009; Le Guerroué and Cozzi, 2010). The second hypothesis proposes that these ultra-low δ^{13}C carbonates are the products of diagenetic re-crystallization of carbonates in the presence of carbon dioxide of organic origin (Vinogradov,

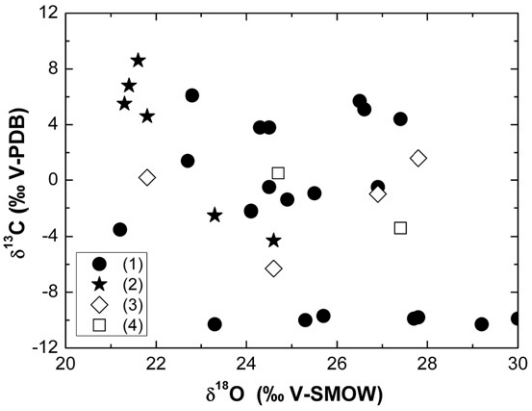

Fig. 2. C–O–isotope cross-plot of dolomites selected for Mg-isotope studies (Pokrovsky and Vinogradov, 1991; Vinogradov et al., 1994; Pokrovsky et al., 2006a; Pokrovsky, 2009; Pokrovsky et al., 2010; this study). 1) Ediacaran of the north and north-east of Patom Paleobasin; 2) Ediacaran of the west of the Patom Paleobasin; 3) Other Ediacaran and Low Cambrian; 4) Mesoproterozoic.

2008; Knauth and Kennedy, 2009; Derry, 2010). However, the carbon isotope shift cannot be linked solely to dolomite formation because dolostones and limestones of unit III have similar $\delta^{13}C$ values (Pokrovsky et al., 2006a). The studied samples do not exhibit any $\delta^{13}C$–$\delta^{18}O$ correlation (Fig. 2). Normally, such a correlation is considered as a straightforward evidence of the diagenetic modification of C- and O-isotopic composition of sedimentary carbonates (Vinogradov, 2008; Knauth and Kennedy, 2009; Derry, 2010). Therefore, in accord with direct geological and mineralogical observations, diagenetic transformation of studied carbonates is considered to be negligible.

A typical feature of Late Neoproterozoic (850–545 Ma) is the very fast increase of $^{87}Sr/^{86}Sr$ ratio in seawater, up to ~0.001/100 Ma (Halverson et al., 2007, 2010; Shields, 2007), which is 10 times higher than the trend observed over the previous 1 billion years (Shields and Veizer, 2002; Shields, 2007). In the least altered high-Sr (up to 24,000 ppm) limestones of the central part of the Patom Paleobasin the ratio $^{87}Sr/^{86}Sr$ increases from 0.7073 to 0.7086 during Ediacaran (Pokrovsky et al., 2006a; Melezhik et al., 2009). This is in agreement with other Sr isotope data for the Neoproterozoic carbonates around the world (Halverson et al., 2010). The stratigraphic rise in $^{87}Sr/^{86}Sr$ from 0.7080 to 0.7086 was observed in several sections of low-^{13}C limestones of unit III (Melezhik et al., 2009). It is believed that the most likely cause of rapid $^{87}Sr/^{86}Sr$ increase in the Neoproterozoic ocean was the increase of silicate weathering which could have been stimulated by the appearance of soil biota (Shields, 2007) or orogenic processes (Melezhik et al., 2009).

Sr isotope data on dolomites (Table 1) are not representative for evolution of the sea water because diagenetic shifts of $^{87}Sr/^{86}Sr$ ratios in the dolomites are, commonly, more significant than those in the limestones due to much lower Sr contents in the dolomites. This difference between dolomite and limestone is rather narrow in most dolomites of NE part of Patom Paleobasin (Table 1). For example, low Sr content dolomite sample No. 1g/384 (Table 1) exhibits the same $^{87}Sr/^{86}Sr$ ratio as high-Sr limestones of unit III (not shown here).

3. Methods

Mg isotope composition of carbonate samples was constrained using a bulk digestion procedure. For this procedure, 10 μg to 20 μg of powdered carbonate sample was reacted with concentrated (16 M) bi-distilled HNO_3 in Teflon reactors heated at 120 °C in the clean room class A 10,000. This allowed maximal leaching of all Mg from dolomite or magnesite matrices, without interferences with silicate admixtures. No pre-leaching with diluted acid was performed because X-ray spectra indicate minor amounts of $CaCO_3$ present in the samples (usually bellow detection limit) and thus the effect of admixtures in the dolomite/magnesite Mg pool is believed to be negligible. Magnesium separation from matrix elements (mainly Ca) was performed using the protocol defined by Teng et al. (2007), in which ~15 μg of Mg were evaporated to dryness and re-dissolved in 2 ml 1 N HNO_3 solution. Later, samples were loaded onto Bio-Rad poly prop 10 ml columns containing AG50W-X12 resin.

Mg isotopes were measured with a Thermo-Finnigan 'Neptune' Multi Collector Inductively Coupled Plasma Mass Spectrometer (MC-ICP-MS) at GET (Toulouse, France). All solutions were prepared in 0.32 M HNO_3 and were introduced into the Ar Plasma using a standard spray chamber. Instrumental mass fractionation effects were corrected using sample-standard bracketing, and all data are presented in delta notation with respect to DSM3 international reference material (Galy et al., 2001):

$$\delta^{x}Mg = \left(\frac{\left(\frac{^{x}Mg}{^{24}Mg}\right)_{sample}}{\left(\frac{^{x}Mg}{^{24}Mg}\right)_{DSM3}} - 1 \right) \cdot 1000. \quad (1)$$

Analytical methods used to determine C, O, and Sr isotope compositions were published previously (Pokrovsky et al., 2006a, 2010). The $\delta^{13}C$ values are given in per mil versus V-PDB and $\delta^{18}O$ versus V-SMOW standards.

4. Results

Measured $\delta^{26}Mg$ and $\delta^{25}Mg$ values range from −2.43‰ to −0.47‰ and from −1.28‰ to −0.26‰, respectively (Table 1). A good correlation between the two Mg isotopic ratios suggests a mass-dependent fractionation process (not shown here). The existing data do not suggest any dependence between Mg isotope composition and depositional age at the interval from ~1500 Ma to 530 Ma. Mesoproterozoic, Neoproterozoic and Low Cambrian dolomites, having "normal sea" $\delta^{13}C = 0 \pm 2‰$, exhibit relatively small variations in $\delta^{26}Mg$ values from −1.62‰ to −2.29‰ and a mean $\delta^{26}Mg = -1.98 \pm 0.23‰$ that is close to the present day carbonate sediment values (Galy et al., 2002; Young and Galy, 2004; Tipper et al., 2006a,b). The dolomites having anomalous high $\delta^{13}C$ values ($5.5 \pm 1.5‰$) can be divided, according to Mg isotopic composition, into two groups. The first group is composed of Neoproterozoic dolomites of the N and NE part of the Patom Paleobasin, having average value of $\delta^{26}Mg$ equal to $2.05 \pm 0.31‰$. The second group is represented by dolomites of the Uluntuy formation, having $\delta^{26}Mg = 1.22 \pm 0.27‰$. Ultra-low $\delta^{13}C$ ($-10.0 \pm 03‰$) dolomite of Torgo Formation exhibit values of $\delta^{26}Mg = 1.03 \pm 0.31‰$. If the fractionation of Mg isotopes between dolomite and seawater was the same as at the present time, it means that the seawater equilibrated with dolomites of Torgo Formation should be at least 1‰ enriched in ^{26}Mg compared to the contemporary value.

No correlation is observed between Mg- and O-isotope compositions (Fig. 3A). In contrast, a strong negative correlation between $\delta^{26}Mg$ and $\delta^{13}C$ values is pronounced in the northern and northeastern part of the Patom Basin (site 1 and 2; Fig. 3B). It can be approximated as:

$$\delta^{26}Mg = -0.072 \cdot \delta^{13}C - 1.83; R^2 = 0.73, n = 20 \quad (2)$$

Within the stratigraphic sequence, all positive C-isotope excursions coincide with negative Mg-isotope shifts and vice versa as it is illustrated in Fig. 4.

Most analyzed samples follow the same trend (Fig. 3B), and the inclusion of most other samples from the Siberian Platform does not appreciably affect this regression with $R^2 = 0.66$ ($n = 28$). The exception is four high-$\delta^{13}C$ dolomites from the Uluntuy Formation of the western part of the Patom Paleobasin (Fig. 1) that yield a positive $\delta^{26}Mg$–$\delta^{13}C$ correlation (Fig. 3B).

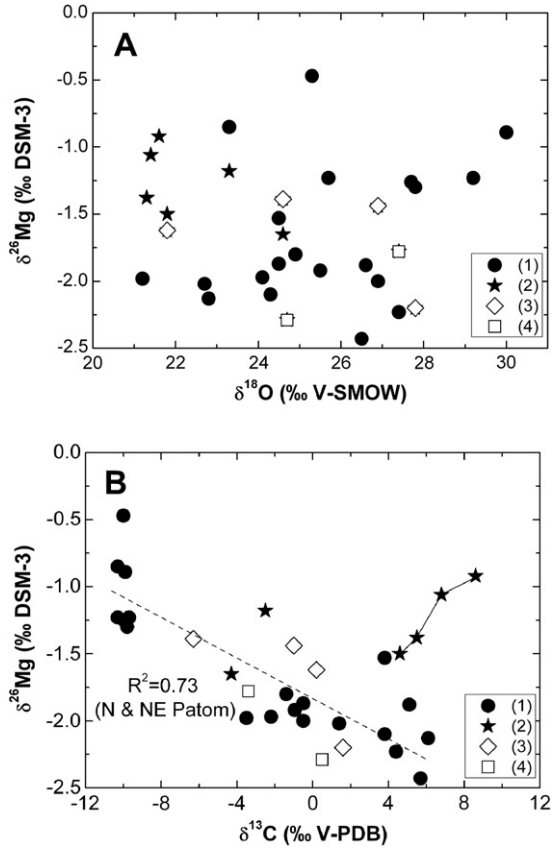

Fig. 3. Relationship between oxygen and magnesium (A) and carbon and magnesium (B) isotope composition in the selected dolomites of the Siberian Platform. 1) Ediacaran of the north and north-east of Patom Paleobasin; 2) Ediacaran of the west of the Patom Paleobasin; 3) Other Ediacaran and Low Cambrian; 4) Mesoproterozoic. A solid line on (B) represents a linear correlation $\delta^{26}Mg = -0.072 \cdot \delta^{13}C - 1.83$; $R^2 = 0.73$, calculated for north and north-east of the Patom Paleobasin (18 points). Most of the other points lie on this regression with $R^2 = 0.66$ (n = 28), excluding 4 samples from the Uluntuy Formation.

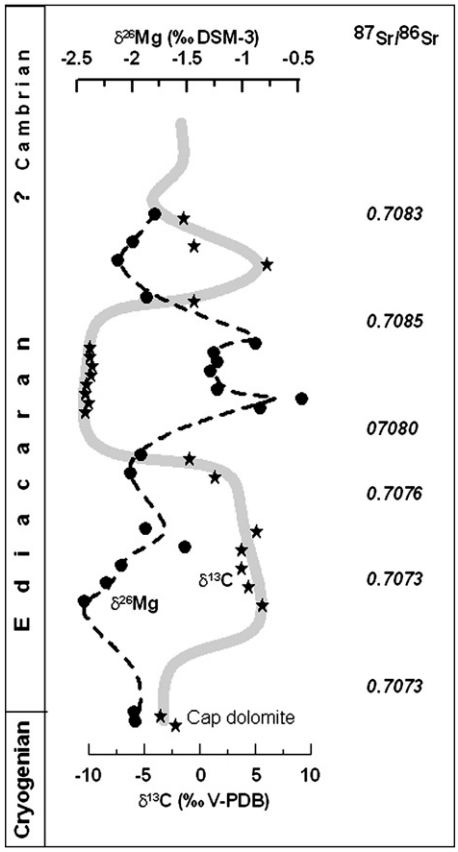

Fig. 4. Secular C (stars, gray line) and Mg (points, dashed line) isotope co-variations in the Ediacaran and Ediacaran–Lower-Cambrian dolostones of N and NE of the Patom Paleobasin. The numbers in the right column represent Sr isotope composition of sub-synchronic high-Sr limestones (Pokrovsky et al., 2006a; Melezhik et al., 2009).

5. Discussion

The correlation between $\delta^{26}Mg$ and $\delta^{13}C$ is an unforeseen and novel result. It is widely accepted that the main reasons for $\delta^{13}C$ variations in sedimentary rocks are separation and secondary mixing of carbon from "organic" and "carbonate" reservoirs. However, the content of "organic" magnesium (linked to organic matter) both in the ocean and in the diagenetic fluids is negligible compared to carbonate magnesium. Oxidation of organic matter, even if it occurs during diagenesis of carbonate sediments rich in organic carbon leading to their re-crystallization and $\delta^{13}C$ decrease, should not bring about a significant shift in Mg isotopic composition at the sedimentation stage. Therefore, the observed correlation may be linked to post-sedimentary (diagenetic) transformations and mineral re-crystallization, and/or actual mineral sedimentation conditions of the Patom Paleobasin. These two possible scenarios are discussed below.

In the case of mineral precipitation from aqueous fluid at low temperatures (diagenetic hypothesis), dolomite is depleted in ^{26}Mg by 2‰ to 2.6‰ (as confirmed by recent ab anitio calculations, Rustad et al., 2010), whereas clay minerals are enriched in ^{26}Mg by 0‰ to 1.25‰ with respect to the fluid (Higgins and Shrag, 2010). The diagenetic solution may become enriched in ^{26}Mg as a result of dolomite precipitation in a restricted water body following a Raleigh fractionation mechanism, or as a result of Mg release due to clay mineral re-crystallization and dehydration.

The Raleigh fractionation may occur in a restricted (water/rock<1) volume of the pore fluid (Higgins and Shrag, 2010). However, a typical amount of early diagenetic dolomite in sediments does not exceed 10% to 15% (Warren, 2000). A 100-m-thick suite of almost pure dolomite may be produced during diagenesis only at very high water/rock (W/R) ratios (>10, or rather >100). A high W/R ratio suggests an almost unlimited external source of Mg that contradicts Raleigh model conditions. According to the second scenario, dolomitization could occur due to massive dehydration and extraction (squeezing) of Mg-rich water from the clay layers during burial diagenesis. In this case, the dolomites of unit III could not preserve a high $\delta^{18}O$, close to the primary $^{87}Sr/^{86}Sr$ ratio and low Mn (Table 1). Within this scenario, it is difficult to explain why only the upper part of unit III at the far northeast of the basin underwent dolomitization. There are very few to no clay deposits in the eastern part of the paleobasin. Therefore, we consider the diagenetic enrichment in ^{26}Mg of ultra-low $\delta^{13}C$ dolomites from unit III very unlikely.

For one series, however, the diagenetic process may become an important factor controlling Mg isotopic composition. Thus, four samples of Uluntuy suite (Ul V_2) do not fit the overall $\delta^{13}C$–$\delta^{26}Mg$ trend (Fig. 3B). In fact, these 4 samples build up a separate positive $\delta^{26}Mg$–$\delta^{13}C$ correlation (Fig. 3B). These samples were collected from relatively thin (10 m to 15 m) horizons of dark gray dolomites hosted in black bituminous limestone that is predominantly in the Uluntuy Formation. The dolomites have relatively low $\delta^{18}O$ values (21.3‰ to 21.8‰) and high Mn content (638 ppm to 1212 ppm) indicating strong diagenetic transformation that probably caused their discordance. Elevated values of $\delta^{26}Mg$ in these samples may stem from organic matter and clay participation in the dolomitization process.

According to the simplified mass balance equation

$$\delta^{13}C_T = F_{c-carb}\delta^{13}C_{carb} + F_{c-org}\delta^{13}C_{org} \quad (3)$$

the sedimentary hypothesis implies that the carbon isotope composition of sedimentary carbonates ($\delta^{13}C_{c\text{-}carb}$) depends on the following 3 parameters: 1) fractions of carbonate carbon ($F_{c\text{-}carb}$) and organic carbon ($F_{c\text{-}org} = 1 - F_{c\text{-}carb}$) buried in sediment; 2) carbon isotope discrimination ($\Delta\delta^{13}C$) between carbonates and organic matter ($\Delta\delta^{13}C = \delta^{13}C_{carb} - \delta^{13}C_{org}$); and 3) total (weighted-average) carbon isotope composition in surface environments ($\delta^{13}C_T$) (Kump et al., 1999; Des Marais, 2001; Ripperdan, 2001; Shields et al., 2002 and references therein). Accordingly:

$$\delta^{13}C_{carb} = \delta^{13}C_T + \left(F_{c-org}\Delta\delta^{13}C\right). \quad (4)$$

However, a similar equation cannot be used for magnesium isotopes because the fraction of organic Mg in sediments is negligible compared to carbonate Mg and does not exceed 0.01 (assuming 8000 ppm Mg in oceanic plankton (Savenko, 1988) and 0.3% organic carbon content in oceanic sediments). Therefore, variations of the $\delta^{26}Mg_{carb}$ should depend on other factors.

At the present time, it is believed that the main sink of Mg in the ocean responsible for removing 80–87% of Mg is hydrothermal exchange between the seawater and oceanic crust whereas carbonate precipitation removes the remaining 10% of Mg pool (Elderfield and Schultz, 1996). Various oceanic basalts and peridotites exhibit homogeneous Mg isotope composition with average value $\delta^{26}Mg_m = -0.25 \pm 0.07$‰ (Teng et al., 2010), about 0.5‰ higher than the seawater ($\delta^{26}Mg_{sw} = -0.82$‰), which is 0.3–0.4‰ heavier than the weighted global Mg-isotope riverine flux to ocean ($\delta^{26}Mg_{rw} = -1.09$‰, Tipper et al., 2006a,b). This difference between $\delta^{26}Mg_{sw}$ and $\delta^{26}Mg_{rw}$ may occur as a result of ~9‰ of dolomite precipitation with $\delta^{26}Mg \sim -2.5$–2.0‰, or due to Mg isotope fractionation during seawater–ocean crust interaction which is poorly known (Tipper et al., 2006b). If hydrothermal fractionation of Mg isotopes is negligible, a variation of $\delta^{26}Mg$ values in seawater through geologic time may depend on: 1) the proportion of hydrothermal to total Mg sink (F_h/F_t), or 2) the change in riverine Mg-isotope flux (Tipper et al., 2006b). Mass balance calculation shows that the decrease of F_h/F_t by a factor of 2 (from 0.9 to 0.4–0.5) should enrich the seawater in ^{26}Mg by ~1‰ (Tipper et al., 2006b). However, such drastic change of hydrothermal activity at the ocean floor or the dolomite sedimentation processes seem very unlikely during Ediacaran which lasted only about 90 Ma. The hydrothermal processes in the ocean are linked to spreading. The rate of spreading in Neoproterozoic is not well constrained. There is no reason to suggest that it was lower than at the present time: the Rodinia continent disintegrated 800–850 Ma ago and during all Neoproterozoic the widening of newly formed oceans occurred (Kheraskova et al., 2010). Although this enlargement probably was discontinuous (Kheraskova et al., 2010), the link of relatively short (several tens Ma) excursions of Ca and Mg isotopic composition in the ocean with variations of the spreading rate seems unlikely. There is also no reason to assume that during Ediacaran, dolomitization and dedolomitization processes were fast and synchronous with the change of carbon isotopic composition. At the Patom Paleobasin, the volume of the ultra-low $\delta^{13}C$ limestones, accumulated during Shuram–Wonoka event is 2 orders of magnitude higher than the ultra-low $\delta^{13}C$, high $\delta^{26}Mg$ dolostones. In this regard, especially important is the analysis of Mg isotope composition in extremely ^{13}C-depleted Ediacaran dolomites of Shuram formation in Oman (Le Guerroué et al., 2006; Le Guerroué and Cozzi, 2010), which is correlated with Torgo formation considered in this study.

As opposed to a negative correlation for Mg and C isotopes documented in this study, a positive link between Ca and C-isotope composition of post Marinoan cap carbonate successions in Namibia, Brazil and NW Canada were recently found (Kasemann et al., 2005; Silva-Tamayo et al., 2010). Considering the long residence time of calcium in the modern ocean (~10^6 years), temporal variations in $\delta^{44}Ca_{sw}$ reflect changes in input of calcium to the ocean from weathering and its removal by carbonate sedimentation (Kasemann et al., 2005; Silva-Tamayo et al., 2010). Indeed, $\delta^{44}Ca$ and $\delta^{13}C$ values decrease when weathering input exceeds sedimentary output ($F_{sw}/F_{sed} > 1$) and increase when $F_{sw}/F_{sed} < 1$.

It is difficult to concede a deficit of Mg in the ocean, taking into account high contents of Mg in seawater and a small amount of Mg-bearing sediments compared to Ca-bearing sediments. We hypothesize that Mg isotope variations in the Late Proterozoic dolomite mainly depend on the predominant type of weathering rocks and the weathering regime, whereas the observed anti-correlation between $\delta^{26}Mg$ and $\delta^{13}C$ is a result of synchronous but not directly linked processes.

It has been shown that the period of high-$\delta^{13}C$ sedimentation coincides with glacioeustatic regressions (Kump et al., 1999; Ripperdan, 2001; Shields et al., 2002) and could be a consequence of increased $\delta^{13}C$ input due to the exposure and weathering of carbonate platforms during sea-level fall. There is little doubt that the high-$\delta^{13}C$ Neoproterozoic carbonates of the Patom Paleobasin (Pokrovsky et al., 2006b), western Mongolia and some other regions (Shields et al., 2002) accumulated under sea regression conditions. At the low ocean level, the carbonate platforms and coastal planes are exposed and subjected to intense weathering. During this time, Mesoproterozoic dolostones that are widespread on the Siberian Platform may become a source of low-$\delta^{26}Mg$ to the ocean. As a result, the ocean would be depleted in $\delta^{26}Mg$, and high-$\delta^{13}C$ carbonates would accumulate during a regression.

Low-$\delta^{13}C$ carbonates of the Patom Paleobasin accumulated during sea transgression (Chumakov, 1959; Bobrov, 1979; Pokrovsky et al., 2006a,b). At a high ocean level, carbonate platforms and coastal planes should be flooded, and the carbonate weathering could be reduced relative to the weathering of igneous and metamorphic silicate rocks. The latter supply the ocean with magnesium that is approximately 1‰ enriched in the heavy isotope (^{26}Mg) compared to carbonates (Galy et al., 2002; Young and Galy, 2004; Tipper et al., 2006a,b). The main cause for this enrichment is that silicate weathering can fractionate Mg isotopes (Tipper et al., 2006a,b; Brenot et al., 2008; Pogge von Strandmann et al., 2008) such that the weathering products are enriched in ^{26}Mg by ~0.5‰ compared to the bedrock. This is contrast to carbonate weathering that does not fractionate Mg isotopes (Jacobson et al., 2010) although the difference of ^{26}Mg between silicate and carbonate rocks is as high as 1.5–2.0‰. As a result, the enrichment of both oceanic water and carbonate sediments by ^{26}Mg could occur during transgression and would coincide with sedimentation of low-^{13}C carbonates. Climate change may be another factor responsible for specific sedimentary environments during sea transgression. Gas-hydrate destabilization due to climate warming is a possible cause of seawater enrichment by the light carbon isotope and sedimentation of both moderately low-^{13}C cap dolomites (Kennedy et al., 2001) and ultra-low carbonates of unit III (Pokrovsky et al., 2006a,b). At the same time, climate warming could be a cause of decreasing riverine $\delta^{26}Mg$ values due to a significant increase in silicate weathering rate with temperature, precipitation and atmospheric CO_2 content increase known to strongly enhance silicate weathering rates (Dessert et al., 2003, 2009).

Available Sr isotope data do not contradict to the suggested link between the Mg isotope composition and the weathering regime. In high-Sr limestones of the Patom Paleobasin $^{87}Sr/^{86}Sr$ ratios rise to 0.7076 at the upper part of unit II (high-^{13}C, low-^{26}Mg) the unit III (low-^{13}C, high-^{26}Mg). Upward in the section, the decreasing of $\delta^{26}Mg$ values from −0.89‰ at the top of unit III to −1.80‰ at the Ediacaran–Lower Cambrian transition strata is correlated with slight decrease of $^{87}Sr/^{86}Sr$ from 0.7086 to 0.7083 (Fig. 4). The presence of anhydrite and halite in the Ediacaran–Lower Cambrian transition strata of Patom Paleobasin and the biggest part of the Siberian Platform witnesses the regressive regime of sedimentation.

6. Conclusions

Until recently, Mg isotope fractionation has been investigated either in experiments or on contemporary or very young geological objects. Our study of ancient (>500 Ma) sedimentary dolomites produced the following unexpected result: a significant negative correlation of Mg and carbon isotopes that could not be anticipated given different geochemical properties of these two elements. Although there is no single and straightforward interpretation of the obtained results, reporting them should stimulate further research.

Most likely, the change in Mg isotope composition in carbonate sediments on a million-year scale is controlled by weathering of carbonate versus silicate rocks. The weathering regime is essentially controlled by the ocean level (transgression–regression cycles) and climate. Similarly, the isotopic composition of carbon also depends on weathering conditions. However, $\delta^{13}C$ variations of Neoprotorozoic rocks are too large to be linked solely to weathering. Burial of organic matter in sediments may also be linked to transgression–regression cycles through various climatic and ocean hydrology mechanisms such as stratification of sedimentation basins and bottom water temperatures. As a result, observed anti-correlation between $\delta^{26}Mg$ and $\delta^{13}C$ does not necessarily prove the existence of functional links in mechanisms controlling the behavior of these two isotopic systems. It can be a result of synchronous (simultaneous) but not directly linked processes.

Acknowledgments

We would like to thank Jerome Chmeleff for his assistance with the MC-ICP-MS analyses in Toulouse. We greatly appreciate the constructive and helpful comments of Adrian Immenhauser and an anonymous reviewer. This work was supported by MC ITN DELTA-MIN (ITN-2008-215360), MC RTN GRASP-CO_2 (MRTN-CT-2006-035868). Financial support from EPOV and INTERVIE INSU programs, LIA LEAGE (France) and by RFBR project 10-05-01061 (Russia) is equally acknowledged.

References

Anbar, A.D., Rouxel, O.J., 2007. Metal stable isotopes in paleoceanography. Annu. Rev. Earth Plan. Sci. 35, 717–746.
Arnold, G.L., Anbar, A.D., Barling, J., Lyons, T.W., 2004. Molybdenum isotope evidence for widespread anoxia in mid-Proterozoic oceans. Science 304, 87–90.
Beard, B., Johnson, C., von Damm, K., Poulson, R., 2003. Iron isotope constraints on Fe cycling and mass balance in oxygenated Earth oceans. Geology 31, 629–632.
Bobrov, A.K., 1979. Stratigraphy and Palaeogeography of Upper Precambrian Deposits of Southern Yakutiya. Yakutiyan Book Publishing, Yakutsk. (in Russian).
Brasier, M.D., Shields, G.S., Kuleshov, V.N., Zhegallo, L.A., 1996. Integrated chemo- and biostratigraphic calibration of early animal evolution: Neoproterozoic–Cambrian of Southern Mongolia. Geol. Mag. 133, 445–485.
Brenot, A., Cloquet, C., Vigier, N., Carignan, J., France-Lanord, C., 2008. Magnesium isotope systematics of the lithologically varied Moselle river basin, France. Geochim. Cosmochim. Acta 72, 5070–5089.
Buhl, D., Immenhauser, A., Smeulders, G., Kabiri, L., Richter, D.K., 2007. Time series $\delta^{26}Mg$ analysis in speleothem calcite: kinetic versus equilibrium fractionation, comparison with other proxies and implications for palaeoclimate research. Chem. Geol. 244, 715–729.
Burns, S.J., Matter, A., 1993. Carbon isotopic record of the latest Proterozoic from Oman. Eclogae Geol. Helv. 86, 595–607.
Chumakov, N.M., 1959. Stratigraphy and tectonics of southeastern part of the Viluy Depression. In: Shatsky, N.S., Tugolesov, D.A., Arsen'ev, A.A. (Eds.), The Tectonics of the USSR, v. IV. Academy of Sciences of the USSR, Moscow, pp. 345–460 (in Russian).
Chumakov, N.M., 1993. Mid-Siberian Riphean glacial horizon. Stratigr. Geol. Correl. 1, 21–34.
Chumakov, N.M., 2011. Glacial deposits of the Nichatka Formation, Chara River basin and review of Upper Precambrian diamictites of Central Siberia. In: Arnaud, E., Halverson, G.P., Shields-Zhou, G.A. (Eds.), The Geologic Record of Neoproterozoic Glaciations. Geological Society, London, Memoirs 36, 297-302.
Chumakov, N.M., Pokrovsky, B.G., Melezhik, V.A., 2007. Geological history of the Patom Complex, Late Precambrian, Central Siberia. Dokl. Earth Sci 413, 355–358.
Chumakov, N.M., Pokrovsky, B.G., Melezhik, V.A., 2011. Glaciogenic Bol'shoy Patom Formation, Lena River, Middle Siberia. In: Arnaud, E., Halverson, G.P., Shields-Zhou, G.A. (Eds.), The Geologic Record of Neoproterozoic Glaciations. Geological Society, London, Memoirs 36, 309-316.
de Villiers, S., Dickson, J.A.D., Ellam, R.M., 2005. The composition of continental weathering flux deduced from seawater Mg isotopes. Chem. Geol. 216, 133–142.
Derry, L.A., 2010. A burial diagenesis origin for Shuram–Wonoka carbon isotope anomaly. Earth Planet. Sci. Lett. 294, 152–162.
Des Marais, D.J., 2001. Isotope evolution of the biogeochemical carbon cycle during the Precambrian. Rev. Mineral. Geochem. 2001 (43), 555–578.
Dessert, C., Dupré, B., Gaillardet, J., François, L.M., Allègre, C.J., 2003. Basalt weathering laws and the impact of basalt weathering on the global carbon cycle. Chem. Geol. 202, 257–273.
Dessert, C., Gaillardet, J., Dupré, B., Schott, J., Pokrovsky, O.S., 2009. Fluxes of high- versus low-temperature water–rock interactions in aerial volcanic areas: the example of the Kamchatka Peninsula, Russia. Geochim. Cosmochim. Acta 73, 148–169.
Elderfield, H., Schultz, A., 1996. Mid-ocean ridge hydrothermal fluxes and the chemical composition of the ocean. Annu. Rev. Earth Planet. Sci. 24, 191–224.
Fike, D.A., Grotzinger, J.P., Pratt, L.M., Summons, R.E., 2006. Oxidation of the Ediacaran ocean. Nature 444, 744–747.
Galy, A., Belshaw, N.S., Halicz, L., O'Nions, R.K., 2001. High-precision measurement of magnesium isotopes by multiple-collector inductively coupled plasma mass spectrometry. Int. J. Mass Spectrom. 208, 89–98.
Galy, A., Bar-Matthews, M., Halicz, L., O'Nions, R.K., 2002. Mg isotopic composition of carbonate: insight from speleothem formation. Earth Planet. Sci. Lett. 201, 105–115.
Grotzinger, J.P., James, N.P., 2000. Precambrian carbonates: evolution of understanding. In: Grotzinger, J.P., James, N.P. (Eds.), Carbonate Sedimentation and Diagenesis in the Evolving Precambrian World. SEPM Special Publication, Tulsa, OK.
Halverson, G.P., Hoffman, P.F., Schrag, D.P., Maloof, A.C., Rice, A.H.N., 2005. Towards a Neoproterozoic composite carbon isotope record. Geol. Soc. Am. Bull. 117, 1181–1207.
Halverson, G.P., Dudas, F.O., Maloof, A.C., Bowring, S.A., 2007. Evolution of the 87Sr/86Sr composition of Neoproterozoic seawater. Palaeogeogr. Palaeoclimatol. Palaeoecol. 256, 103–129.
Halverson, G.P., Wade, B.P., Hurtgen, M.T., Barovich, K.M., 2010. Neoproterozoic chemostratigraphy. Precambrian Res. 182, 337–350.
Higgins, J.A., Shrag, D.P., 2010. Constraining magnesium cycling in marine sediments using magnesium isotopes. Geochim. Cosmochim. Acta 74, 5039–5053.
Hoffman, P.F., 2011. Strange bedfellows: glacial diamictite and cap carbonate from the Marinoan (635 Ma) glaciation in Namibia. Sedimentology 58, 57–119.
Hoffman, P.F., Kaufman, A.J., Halverson, G.P., Schrag, D.P., 1998. A Neoproterozoic snowball earth. Science 281, 1342–1346.
Hoffman, P.F., Halverson, G.P., Domack, E.W., Husson, J.M., Higgins, J.A., Schrag, D.P., 2007. Are basal Ediacaran (635 Ma) post-glacial "cap dolostones" diachronous? Earth Planet Sci. Lett. 258, 114–131.
Immenhauser, A., Buhl, D., Richter, D., Niedermayr, A., Riechelmann, D., Dietzel, M., Schulte, U., 2010. Magnesium-isotope fractionation during low-Mg calcite precipitation in a limestone cave — field study and experiments. Geochim. Cosmochim. Acta 74, 4346–4364.
Jacobsen, S.B., Kaufman, A.J., 1999. The Sr, C and O isotopic evolution of Neoproterozoic seawater. Chem. Geol. 161, 37–57.
Jacobson, A.D., Zhang, Z.F., Lundstrom, C., Huang, F., 2010. Behavior of Mg isotopes during dedolomitization in the Madison Aquifer, South Dakota. Earth Planet. Sci. Lett. 297, 446–452.
Jiang, G.Q., Kennedy, M.J., Christie-Blick, N., 2003. Stable isotopic evidence for methane seeps in Neoproterozoic postglacial cap carbonates. Nature 426, 822–826.
Jiang, G.Q., Kaufman, A.J., Christie-Blick, N., Zhang, S.H., Wu, H.C., 2007. Carbon isotope variability across the Ediacaran Yangtze platform in South China: implications for a large surface-to-deep ocean delta C-13 gradient. Earth Planet. Sci. Lett. 261, 303–320.
Kasemann, S.A., Hawkesworth, C.J., Prave, A.C., Fallick, A.E., Pearson, P.N., 2005. Boron and calcium isotope composition in Neoproterozoic carbonate rocks from Namibia: evidence for extreme environmental change. Earth Planet. Sci. Lett. 231, 73–86.
Kasemann, S.A., Prave, A.R., Fallick, A.E., Hawkesworth, C.J., Hoffmann, K.H., 2010. Neoproterozoic ice ages, boron isotopes, and ocean acidification: implications for a snowball Earth. Geology 38, 775–778.
Kaufman, A.J., Knoll, A.H., 1995. Neoproterozoic variations in the C-isotopic composition of seawater: stratigraphic and biogeochemical implications. Precambrian Res. 73, 27–49.
Kennedy, M.J., Christie-Blick, N., Prave, A.R., 2001. Carbon isotopic composition of Neoproterozoic glacial carbonates as a test of paleoceanographic models for snowball Earth phenomena. Geology 29, 1135–1138.
Kheraskova, T.N., Bush, V.A., Didenko, A.N., Samygin, S.G., 2010. Breakup of Rodinia and early stages of evolution of the Paleoasian ocean. Geotectonics 44, 3–24.
Khomentovskii, V.V., Kochnev, B.B., 1999. Vendian of the Baikal–Patom Depression, Southern Siberia. Geol. Geofiz. 40, 807–822.
Knauth, L.P., Kennedy, M.J., 2009. The late Precambrian greening of the Earth. Nature 460, 728–732.
Knoll, A.H., Hayis, J.M., Kaufman, A.J., Swett, K., Lambert, I.B., 1986. Secular variation in carbon isotope ratios from upper Proterozoic successions of Svalbard and East Greenland. Nature 321, 832–838.
Knoll, A.H., Bambach, R.K., Canfield, D., Grotzinger, J.P., 1996. Late Permian extinctions — reply. Science 274, 1551–1552.
Krupenin, M.T., Chernova, L.C., Kotliarov, V.A., Guliaeva, T.Y., Petrischeva, V.G., 2008. Types of sedimentogenes and lithogenes and their evolution in the Earth history. Proceedings 5-th Russian Lithologic Conference O.V. Yapaskurt & A.V. Maslov (eds.). Ekaterinburg 1, 381–382.
Kump, L.R., Arthur, M.E., Patzkovsky, M.E., Gibbs, D.S., Pinkus, D.S., Sheehan, P.M., 1999. A weathering hypothesis for glaciations at high pCO_2 during the Late Ordovician. Paleogeogr. Paleoclim. Paleoecol. 152, 173–187.
Le Guerroué, E., Cozzi, A., 2010. Veracity of Neoproterozoic negative C-isotope values: the termination of the Shuram negative excursion. Gondwana Res. 17, 653–661.

Le Guerroué, E., Allen, P.A., Cozzi, A., Etienne, J.L., Fanning, M., 2006. 50 Myr recovery from the largest negative $\delta^{13}C$ excursion in the Ediacaran ocean. Terra Nova 18, 147–153.

Magaritz, M., Holser, W.T., Kirschvink, J.L., 1986. Carbon-isotope events across the Precambrian/Cambrian boundary on the Siberian Platform. Nature 320, 258–259.

Melezhik, V.A., Fallick, A.E., Pokrovsky, B.G., 2005. Enigmatic nature of thick sedimentary carbonates depleted in ^{13}C beyond the canonical mantle value: the challenges to our understanding of the terrestrial carbon cycle. Precambrian Res. 137, 131–165.

Melezhik, V.A., Pokrovsky, B.G., Fallick, A.E., Kuznetsov, A.B., Bujakaite, M.I., 2009. Constraints on Sr-87/Sr-86 of Late Ediacaran seawater: insight from Siberian high-Sr limestones. J. Geol. Soc. 166, 183–191.

Nedelec, A., Affaton, P., France-Lanord, C., Charriere, A., Alvaro, J., 2005. Sedimentology and chemostratigraphy of the Bwipe Neoproterozoic cap dolostones (Ghana, Volta Basine): a record of microbial activity in peritidal environment. C.R. Geosci. 339, 516–518.

Pelechaty, S.M., 1998. Integrated chemostratigraphy of the Vendian System of Siberia: implications for a global stratigraphy. J. Geol. Soc. (London, U.K.) 155, 957–973.

Pogge von Strandmann, P.A.E., James, R.H., van Calsteren, P., Gislason, S.R., Burton, K.W., 2008. Lithium, magnesium and uranium isotope behaviour in the estuarine environment of basaltic islands. Earth Planet. Sci. Lett. 274, 462–471.

Pokrovsky, B.G., 1996. The Proterozoic–Palaeozoic boundary: isotope anomalies in the Siberian Platform sections and global environmental changes. Lithol. Min. Res. 31, 333–347.

Pokrovsky, B.G., 2009. Traces of brine and hydrocarbon migration in carbon, oxygen, and sulfur isotopic compositions of reservoir rocks in the Talakan petroleum field, Southwestern Yakutia. Lithol. Min. Res. 44, 258–266.

Pokrovsky, B.G., Vinogradov, V.I., 1991. Isotopic Compositions of Strontium, Oxygen, and Carbon in Upper Precambrian Carbonates from the Anabar Highland. Dokl. Akad. Nauk SSSR 320, 1245–1250.

Pokrovsky, B.G., Chumakov, N.M., 2008. Ultra high and ultra low $\delta^{13}C$ Neoproterozoic carbonates at the Baikal–Patom Depression and some other regions of the Siberia and Ural. Proceed. V Lithological Conference, Ekaterinburg, pp. 172–175 (in Russian).

Pokrovsky, B.G., Gertsev, D.O., 1993. Upper Precambrian carbonates extremely depleted in ^{13}C. Lithol. Min. Res. 1, 64–80.

Pokrovsky, B.G., Melezhik, V.A., Bujakaite, M.I., 2006a. Carbon, oxygen, strontium, and sulfur isotopic compositions in Late Precambrian rocks of the Patom Complex, Central Siberia: communication 1. Results, isotope stratigraphy, and dating problems. Lithol. Min. Res. 41, 450–474.

Pokrovsky, B.G., Melezhik, V.A., Bujakaite, M.I., 2006b. Carbon, oxygen, strontium, and sulfur isotopic compositions in Late Precambrian rocks of the Patom Complex, Central Siberia: communication 2. Nature of carbonates with ultralow and ultrahigh $\delta^{13}C$ values. Lithol. Min. Res. 41, 576–587.

Pokrovsky, B.G., Chumakov, N.M., Melezhik, V.A., Bujakaite, M.I., 2010. Geochemical properties of Neoproterozoic "cap dolomites" in the Patom paleobasin and problem of their genesis. Lithol. Min. Res. 45, 577–592.

Pustylnikov, A.M., Bogdanova, V.N., Vakulenko, L.G., 1989. Lithology and sedimentation environment of carbonates of Oskoba Formation. Proceedings of Inst. Geology and Geophisic. Novosibirsk, pp. 105–117 (in Russian).

Ripperdan, R.L., 2001. Stratigraphic variation in marine carbonate carbon isotope ratios. Rev. Mineral. Geochem. 43, 637–662.

Rustad, J.R., Casey, W.H., Yin, Q.Z., Bylaska, E.J., Felmy, A.R., Bogatko, S.A., Jackson, V.E., Dixon, D.A., 2010. Isotopic fractionation of $Mg^{2+}(aq)$, $Ca^{2+}(aq)$, and $Fe^{2+}(aq)$ with carbonate minerals. Geochim. Cosmochim. Acta 74, 6301–6323.

Salop, L.M., 1964. Geology of Baikalian mounting region. Nauka, Moscow. (in Russian).

Savenko, V.S., 1988. Elementary composition of oceanic plankton. Geochem. Int. 8, 1084–1089.

Schauble, E.A., 2010. First-principles estimates of equilibrium magnesium isotope fractionation in silicate, oxide, carbonate and hexaaquamagnesium(2+) crystals. Geochim. Cosmochim. Acta 75, 844–869.

Severmann, S., Lyons, T.W., Anbar, A., McManus, J., Gordon, G., 2008. Modern iron isotope perspective on the benthic iron shuttle and the redox evolution of ancient oceans. Geology 36, 487–490.

Shen, Y., Zhang, T., Chu, X.C., 2005. Isotopic stratification in a Neoproterozoic postglacial ocean. Precambr. Res. 137, 243–251.

Shields, G.A., 2005. Neoproterozoic cap carbonates: a critical appraisal of existing models and the plumeworld hypothesis. Terra Nova 17, 299–310.

Shields, G.A., 2007. A normalized seawater strontium isotope curve: possible implications for Neoproterozoic–Cambrian weathering rates and the further oxygenation of the Earth. eEarth 2, 35–42.

Shields, G.A., Veizer, J., 2002. Precambrian marine carbonate isotope database: Version 1.1. Geochem. Geophys. Geosyst. 6, 1–12.

Shields, G.A., Brasier, M.D., Stille, S., Dorjnamjaa, D., 2002. Factors contributing to high $\delta^{13}C$ values in Cryogenian limestones of western Mongolia. Earth Planet. Sci. Lett 196, 99–111.

Silva-Tamayo, J.C., Nagler, T.F., Sial, A.N., Nogueira, A., Kyser, K., Riccomini, C., James, N.P., Narbonne, G.M., Villa, I.M., 2010. Global perturbation of the marine Ca isotopic composition in the aftermath of the Marinoan global glaciation. Precambr. Res. 182, 373–381.

Teng, F.Z., Wadhwa, M., Helz, R.T., 2007. Investigation of magnesium isotope fractionation during basalt differentiation: implications for a chondritic composition of the terrestrial mantle. Earth Planet. Sci. Lett. 261, 84–92.

Teng, F.-Z., Li, W.-Y., Ke, S., Marty, B., Dauphas, N., Huang, S., Wu, F.-Y., Pourmand, A., 2010. Magnesium isotopic composition of the Earth and chondrites. Geochim. Cosmochim. Acta 74, 4150–4166.

Tipper, E.T., Galy, A., Bickle, M.J., 2006a. Evidence for a fractionated reservoir of Ca and Mg on the continents: implications for the oceanic Ca cycle, Earth Planet. Sci. Lett. 247, 267–279.

Tipper, E.T., Galy, A., Gaillardet, J., Bickle, M.J., Elderfield, H., Carder, E.A., 2006b. The magnesium isotope budget of the modern ocean: constraints from riverine magnesium isotope ratios. Earth Planet. Sci. Lett. 250, 241–253.

Vieira, L.C., Trindade, R.I.F., Afonso, C.R., Nogueira, A.C.R., Ader, M., 2007. Identification of a Sturtian cap carbonate in the Neoproterozoic Sete Lagoas carbonate platform, Bambuı' Group, Brazil. C. R. Geosci. 339, 240–258.

Vinogradov, V.I., 2008. Carbon and oxygen isotopic composition of the Vendian–Cambrian carbonate rocks and paleoecological reconstructions. Lithol. Min. Res. 43, 44–57.

Vinogradov, V.I., Pokrovsky, B.G., Pustylnikov, A.M., Muravev, V.I., Shatsky, G.V., Buyakaite, M.I., Lukanin, A.O., 1994. Isotopic and geochemical peculiarities and age of Upper-Precambrian deposits in the western part of Siberian craton. Lithol. Min. Res. 29, 349–371.

Walter, M.R., Veevers, J.J., Calver, C.R., Gorjan, P., Hill, A.C., 2000. Dating the 840–544 Ma Neoproterozoic interval by isotopes of strontium, carbon, and sulfur in seawater and some interpretative models. Precambrian Res. 100, 371–433.

Warren, J., 2000. Dolomite: occurrence, evolution and economically important associations. Earth Sci. Rev. 52, 1–81.

Young, E.D., Galy, A., 2004. The isotope geochemistry and cosmochemistry of Mg. Rev. Min. Geochem. 55, 197–230.

Zhu, M.Y., Zhang, J.M., Yang, A.H., 2007. Integrated Ediacaran (Sinian) chronostratigraphy of South China. Palaeogeogr. Palaeoclimatol. Palaeoecol. 254, 7–61.